Influence of the A-site cation in $AMnO_{3+x}$ and $AFeO_{3+x}$ (A = La, Pr, Nd and Gd) perovskite-type oxides on the catalytic activity for methane combustion

P.E. Marti

Department of Combustion Technology, Paul Scherrer Institut, CH-5232 Villigen PSI, Switzerland

and

A. Baiker [1]

Department of Chemical Engineering and Industrial Chemistry, Swiss Federal Institute of Technology, ETH-Zentrum, CH-8092 Zurich, Switzerland

Received 1 December 1993; accepted 8 February 1994

The effect of rare-earth ions (La, Pr, Nd and Gd) in $AMnO_{3+x}$ and $AFeO_{3+x}$ perovskites on the thermal behavior and on the catalytic activity for the deep oxidation of methane has been studied. $AMnO_{3+x}$ perovskites showed after preparation an oxidative non-stoichiometry. Oxygen desorption analysis revealed for the four manganites different desorption steps occurring between 930 and 1370 K. Stoichiometry was reached after the first desorption step. Heating the samples at temperatures above 1300 K resulted in phase segregation to the simple oxides. $AFeO_{3+x}$ perovskites were more stable towards thermal decomposition than the Mn-perovskites, showing no oxygen evolution up to 1400 K. The reducibility of these perovskites in hydrogen correlated inversely with the relative effective ionic radii of the trivalent rare-earth cations. Comparative catalytic studies were carried out in a fixed-bed microreactor at atmospheric pressure in the temperature range 600–1200 K. The activities at 770 K, expressed as reaction rates referred to the BET surface area, varied between 1.4×10^{-7} and 2.9×10^{-7} mol s^{-1} m^{-2} for the $AMnO_{3+x}$, and between 1.1×10^{-7} and 1.6×10^{-7} mol s^{-1} m^{-2} for the $AFeO_{3+x}$ perovskites.

Keywords: methane combustion; $AMnO_{3+x}$; $AFeO_{3+x}$; perovskites; oxidative non-stoichiometry; TPD of oxygen

1. Introduction

New combustion technologies have been investigated in recent years in order to reduce the emission of pollutants during the combustion of hydrocarbons. Cat-

[1] To whom correspondence should be addressed.

alytic combustion and catalytically stabilized thermal combustion have been proposed [1–3] as efficient methods for reducing the thermal NO_x production. Catalytic combustion devices with high heat throughput, such as gas turbines or industrial burners require active and thermal stable catalysts [4,5]. These properties can be found in some perovskite-type oxides with the general formula ABO_3, which contain a lanthanide in the A position and a transition metal in the B position.

Previous studies [6,7] revealed that $LaCoO_3$, $LaNiO_3$, $LaMnO_3$ and $LaFeO_3$ belong to the more active complex oxides for the methane combustion. An interesting characteristic of rare-earth perovskites is the possibility to vary the dimensions of the unit cell by varying the A ion, and thereby the covalence of the B–O bond in the ABO_3 structure. A thorough study of the role of the A- and B-site ions on the catalytic properties of ABO_3 perovskites for the oxidation of propane and methanol has been reported by Nitadori et al. [8]. They concluded that the influence of the rare-earth ions in the A-site on the oxidation properties of these compounds were secondary, as long as they were trivalent. Zhang et al. [9] studied the oxygen sorption and catalytic properties, for the methane and *n*-butane combustion, of $La_{1-x}Sr_xCo_{1-y}Fe_yO_3$. Whilst the catalytic activity for the *n*-butane oxidation was affected by the transition-metal substitution as well as by the rare-earth substitution, the catalytic activity for the methane oxidation was only influenced by the rare-earth ion substitution. In a previous study [10] we have found that the activity of $ACoO_3$ oxides for the methane oxidation was, with exception of the $PrCoO_3$ perovskite, only slightly influenced by the A-site cations.

In the present work we have investigated the effects of the rare-earth ions in $AMnO_{3+x}$ and $AFeO_{3+x}$ perovskite-type oxides, focusing on the structural properties, oxygen desorption, reduction, thermal stability and on the catalytic activity for methane oxidation. Powder X-ray diffraction, thermogravimetry, gas adsorption and oxygen evolution measurements have been used to pursue this aim.

2. Experimental

2.1. CATALYSTS

The catalysts were prepared by calcination of water-insoluble hydroxide mixtures, using freshly calcined (570 K) simple oxides as precursor materials, La_2O_3, Pr_6O_{11}, Nd_2O_3 and Gd_2O_3, from Fluka (puriss), and Mn_2O_3 from Alfa Products (98%). $Fe(NO_3)_3 \cdot 9H_2O$ (Fluka, puriss) was used for the preparation of the $AFeO_3$ samples. Rare-earth oxides (0.0165 mol, referred to the cation) were dissolved in a solution of nitric acid (5 M, 12 ml). The dissolution of Mn_2O_3 (0.0165 mol, referred to the cation) in concentrated nitric acid was facilitated by dropwise addition of H_2O_2. The volume of the solution was completed to 100 ml with deionized water and added dropwise together with an aqueous solution of tetramethylammonium hydroxide (2.8 M, Fluka, pract.) to 100 ml of deionized water at 300 K and

at a constant pH of 9.0, with vigorous stirring. The precipitated hydroxides were separated from the liquid by centrifugation and washed twice with deionized water. Barnard et al. [11] have reported for $LaCoO_3$ that samples which were washed with acetone before dehydration had higher surface areas than samples which were directly dehydrated by air-drying. Based on this experience the precipitate was washed with acetone before drying at 400 K in air and subsequently calcined in air at 1070 K for 10 h and finally at 1170 K for 12 h. The catalysts were pressed, crushed and sieved. The size fraction between 100 and 300 μm was used for catalytic tests and nitrogen physisorption measurements.

2.2. PHYSICOCHEMICAL CHARACTERIZATION

Phase identification of the catalysts was carried out by powder X-ray diffractometry using a Siemens D5000 diffractometer. Conditions were: Cu K_α radiation, 20 mA, 25 kV, Ni-filter, step scan size = 0.0009°. The patterns obtained were compared with JCPDS data files.

Physisorption measurements were performed with a Micromeritics ASAP 2000 instrument. The BET surface areas were determined by nitrogen adsorption at 77 K in the relative pressure range $0.05 \leqslant p/p^0 \leqslant 0.20$ assuming a cross-sectional area of 0.162 nm^2 for the nitrogen molecule. Before the adsorption measurements the samples were outgassed in vacuum at 423 K for 4 h.

Thermoanalytical investigations were carried out using a Mettler thermoanalyzer (TA 2000 C). Approximately 15 mg of the sample were placed in a platinum sample pan and heated at 10 K/min from room temperature to 1270 K. High purity gases (Ar: 99.998, H_2: 99.999) were passed through the sample chamber (25 ml/min) at atmospheric pressure. As a reference α-Al_2O_3 was used.

Temperature-programmed desorption (TPD) of oxygen was measured in a flow system. Each sample (0.100 g) was placed in a fused-quartz microreactor and pretreated in air (300 ml/min STP) at 1120 K for 1 h. The sample was then cooled to room temperature in the same atmosphere and subsequently heated in a He stream (300 ml/min STP) at a constant heating rate of 10 K/min. The evolving oxygen was monitored with an on-line quadrupole mass spectrometer (Balzers GAM 445).

2.3. CATALYTIC TESTS

Kinetic studies were performed in a continuous fixed-bed microreactor operated at atmospheric pressure. The reactor was a 6 mm o.d. and 4 mm i.d. fused-quartz tube, placed vertically in an electric furnace. The catalyst temperature was monitored by a chromel–alumel thermocouple separated from the catalyst bed by a 0.2 mm thick quartz wall. To preheat the reactant gases and to obtain a uniform velocity profile, quartz-wool was placed before and after the catalyst bed. The reactant feed rate was controlled by mass flow controllers (Brooks 5850E). Both inlet

and outlet gas compositions were quantitatively analyzed using an on-line quadrupole mass spectrometer (Balzers GAM 445).

Comparative activity tests were carried out under the following conditions: reactant feed, 1% CH_4 (99.995%), 4% O_2 (99.999%) and 95% He (99.998%); catalyst load, 0.100 g mixed with 0.100 g SiO_2 powder to reduce the heat release per unit volume; the gas flow rate was adjusted to achieve a gas hourly space velocity (GHSV) of 135 000 h^{-1}. The temperature was increased stepwise from 570 to 1150 K. Reported activities are steady-state values measured after steady-state conversion has been attained. After completion of the whole test series the measurement at 870 K was repeated to confirm the stationarity of the catalyst activity during the kinetic test. The methane conversion to CO_2 was calculated from a carbon balance: $P_{CO_2}/(P_{CH_4} + P_{CO_2} + P_{CO}) \times 100$, where P_{CH_4}, P_{CO_2} and P_{CO} are the partial pressures of CH_4, CO_2 and CO respectively.

3. Results

3.1. BULK STRUCTURE AND PHYSISORPTION MEASUREMENTS

The formation of the perovskite phase was confirmed by XRD, the patterns are shown in fig. 1 ($AMnO_{3+x}$) and in fig. 2 ($AFeO_{3+x}$), respectively. The reflections

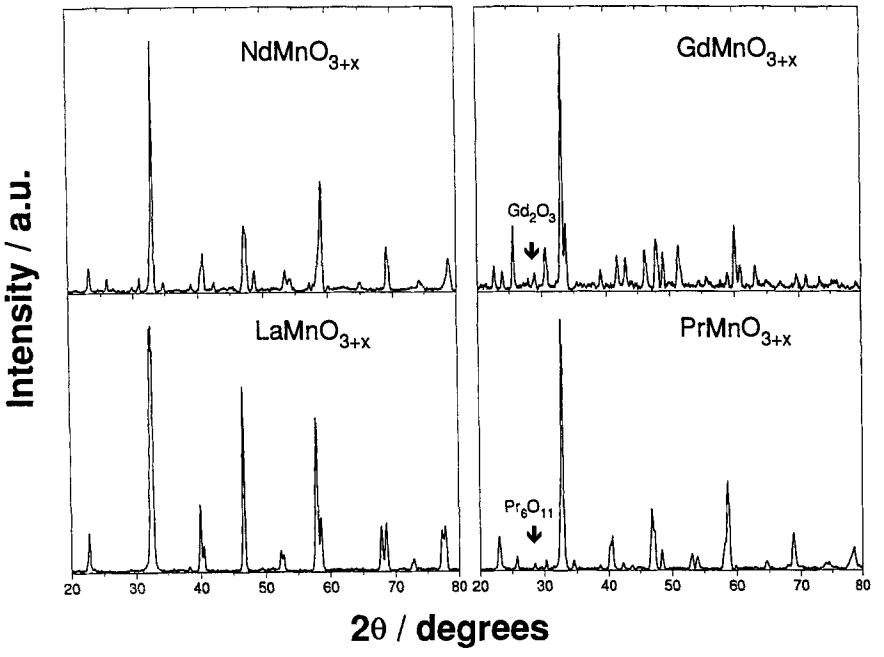

Fig. 1. XRD powder patterns (Cu K_α) of the $AMnO_{3+x}$ perovskites. Arrows mark reflections of the impurities (Pr_6O_{11} and Gd_2O_3).

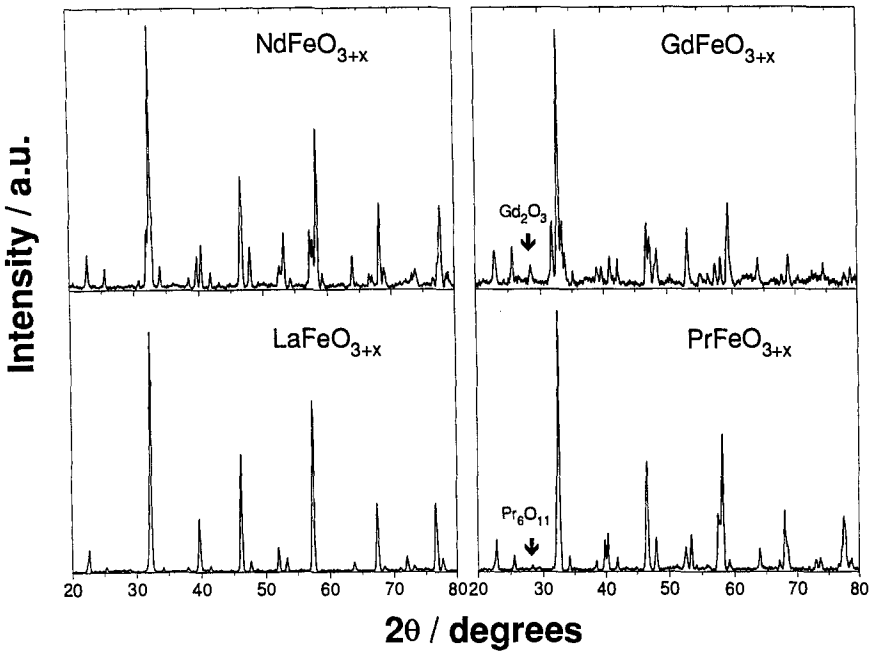

Fig. 2. XRD powder patterns (Cu K_α) of the $AFeO_{3+x}$ perovskites. Arrows mark reflections of the impurities (Pr_6O_{11} and Gd_2O_3).

of the $LaMnO_{3+x}$ sample correspond to the non-stoichiometric phase $LaMnO_{3.15}$, as a comparison with the JCPDS data file (32-0484) reveals. Wold and Arnott [12] reported an oxidative non-stoichiometry in $LaMnO_{3+x}$ varying between $x = 0$ and $x = 0.15$. They also found a change in the symmetry of $LaMnO_{3+x}$ from orthorhombic to rhombohedral when the non-stoichiometry (x) exceeded 0.105.

The XRD pattern of $GdMnO_{3+x}$ corresponds to the JCPDS data file of $GdMnO_{3.00}$ (25-0337). The $GdMnO_{3+x}$ and $GdFeO_{3+x}$ samples contain as a second phase Gd_2O_3. To determine roughly the content of this impurity, two mechanical mixtures of perovskite with 5, respectively, 10 wt% Gd_2O_3 were prepared and analyzed by means of X-ray diffraction. The corresponding XRD pattern revealed that in both perovskites the Gd_2O_3 content should be less than 5 wt%. The $PrMnO_{3+x}$ and $PrFeO_{3+x}$ samples contained traces of Pr_6O_{11}.

No major differences in the morphological properties of the samples emerged from the nitrogen sorption data. For all samples type IV isotherms with very little hysteresis (type H1, according to the IUPAC classification [13]) were observed at high relative pressures. The t-plots confirmed the absence of micropores. BET surface areas are listed in table 1.

3.2. TEMPERATURE-PROGRAMMED DESORPTION OF OXYGEN FROM $AMnO_{3+x}$

The thermal behavior of the $AMnO_{3+x}$ perovskites was examined by TPD of

Table 1
BET surface areas and kinetic results of the investigated catalysts

Catalyst	SA [a] ($m^2\ g^{-1}$)	E_a [b] ($kJ\ mol^{-1}$)	$T_{50\%}$ [c] (K)	Reaction rate [d] ($\mu mol\ s^{-1}\ m^{-2}$)
$LaMnO_{3+x}$	8.0	82 ± 2	955	0.14
$PrMnO_{3+x}$	2.5	89 ± 2	984	0.23
$NdMnO_{3+x}$	2.4	83 ± 1	968	0.29
$GdMnO_{3+x}$	5.3	79 ± 2	950	0.16
$LaFeO_{3+x}$	3.5	105 ± 2	951	0.11
$PrFeO_{3+x}$	5.8	86 ± 4	990	0.15
$NdFeO_{3+x}$	4.5	109 ± 9	991	0.11
$GdFeO_{3+x}$	5.6	89 ± 2	980	0.16

[a] BET surface areas determined by nitrogen adsorption.
[b] Apparent activation energy with 95% confidence limits.
[c] Temperature at which 50% methane conversion was attained.
[d] Calculated at 770 K.

oxygen. Fig. 3 depicts the TPD profiles, the oxygen evolution rate is plotted as a function of the catalyst temperature. The perovskites show a first desorption peak between 925 K ($PrMnO_{3+x}$) and 1250 K ($NdMnO_{3+x}$), which overlaps with a sec-

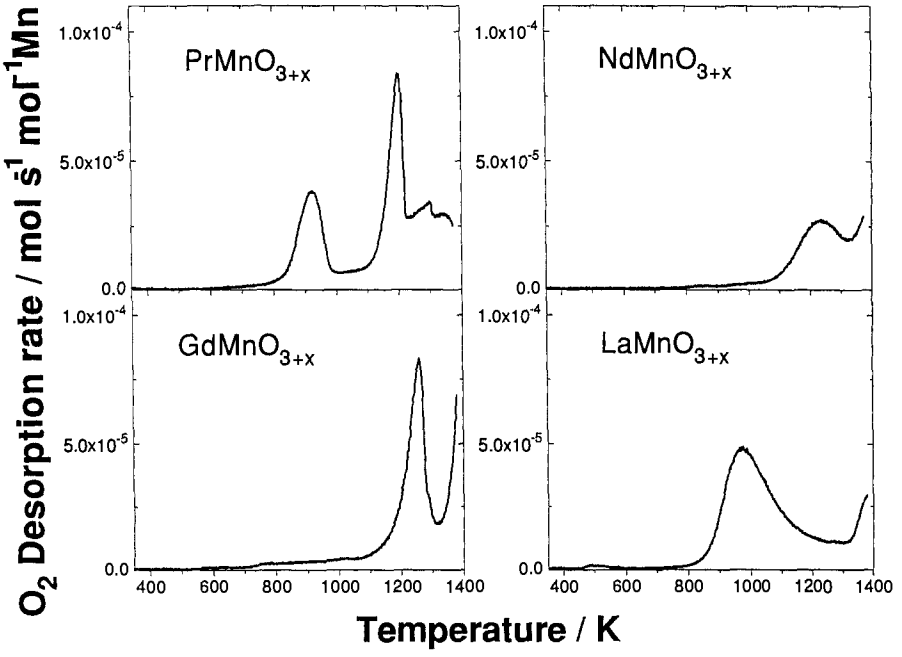

Fig. 3. Temperature-programmed oxygen evolution from $AMnO_3$ perovskites. Sample weight: 0.1 g, carrier gas: He (300 ml/min), heating rate: 10 K/min.

ond one beginning around 1300 K. The $PrMnO_{3+x}$ sample exhibits a more complex desorption behavior, with more than two distinct desorptions.

To check whether the samples were contaminated with Mn_2O_3, the oxygen evolution from Mn_2O_3 was measured. It showed a single desorption peak at 1050 K, where no desorption maximum is observed with $AMnO_{3+x}$.

Table 2 lists the amounts of oxygen which desorbed from the samples during the TPD experiments. These amounts were calculated by integrating the oxygen desorption rate with time.

Fig. 4 shows the XRD patterns of the samples after thermal treatment in He up to completion of the corresponding first desorption step. A comparison of the results presented in figs. 1 and 4 reveals clearly a structural change of the perovskites, with exception of the $GdMnO_{3+x}$ sample. The XRD patterns of these samples agree with the JCPDS data files of the corresponding stoichiometric compounds ($LaMnO_{3.00}$: 35-1353, $NdMnO_{3.00}$: 25-0565). For $PrMnO_{3.00}$ no JCPDS data file was available, so that a simulation of the powder XRD pattern with the program Pulverix, using the lattice parameters given by Quezel-Ambrunaz [14], was carried out. The calculated pattern agreed well with the measured pattern.

3.3. THERMAL BEHAVIOR OF $AFeO_3$ IN HYDROGEN

The $AFeO_3$ samples showed no significant oxygen evolution in the temperature range 300–1400 K, so that their reduction behavior was studied under a hydrogen atmosphere using TG (table 3). Under the experimental conditions used (heating rate 10 K/min, pure H_2), the reduction occurred with all samples in two steps.

Table 2
Characteristic data of oxygen desorption measurements from $AMnO_{3+x}$

Catalyst	T_{max} [a] (K)	$T_{interval}$ [b] (K)	Amount oxygen evolved [c] (mmol mol^{-1} Mn)
$LaMnO_{3+x}$	970	600–1300	69
		1300–1370	7
$PrMnO_{3+x}$	925	600–1000	25
	1200	1000–1260	33
		1260–1370	32
$NdMnO_{3+x}$	1240	600–1310	29
		1310–1370	8
$GdMnO_{3+x}$	1260	600–1300	50
		1300–1370	14

[a] Temperature at which the oxygen desorption rate reached a maximum.
[b] Temperature interval used for the integration.
[c] Oxygen which evolved from 0.1 g sample into 300 ml/min He at a heating rate of 10 K/min following treatment at 1120 K in air for 1 h.

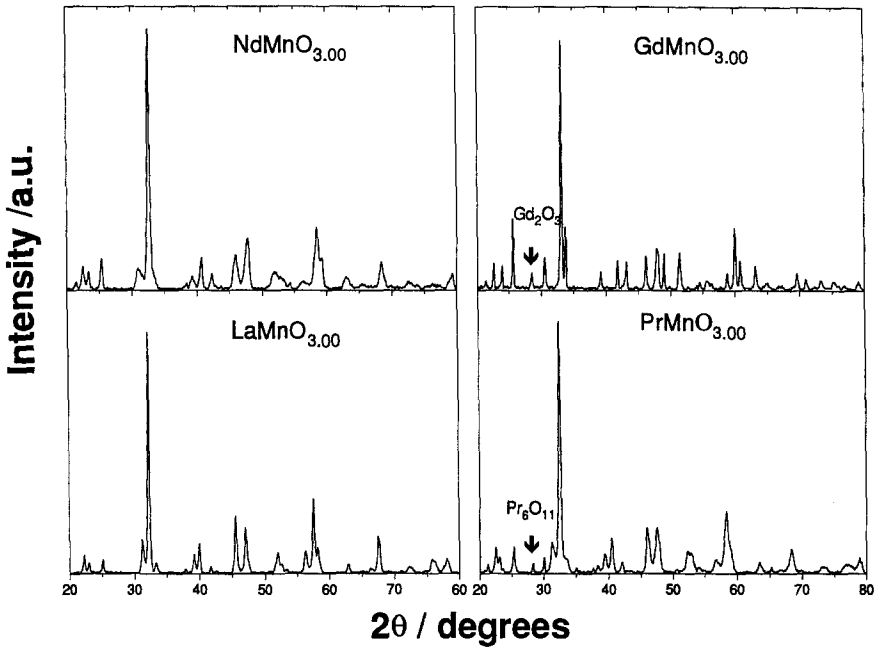

Fig. 4. XRD patterns of $AMnO_3$ catalysts after the first oxygen evolution peak during the TPD experiments, i.e., after heating them in He up to 1300 K ($LaMnO_3$, $NdMnO_3$ and $GdMnO_3$) or 1000 K ($PrMnO_3$).

Table 3
Results of the reduction of $AFeO_{3+x}$ in pure hydrogen atmosphere

Catalyst	$T_{interval}$ [a] (K)	Weight loss [b] (%)	Change in the non-stoichiometry [c] (as δ in $AFeO_{3+x-\delta}$)
$LaFeO_{3+x}$	760–940	1.98	0.30
	1120–		
$PrFeO_{3+x}$	840–960	0.71	0.11
	1060–		
$NdFeO_{3+x}$	680–710	0.45	0.07
	990–1220	8.97	1.39
$GdFeO_{3+x}$	850–970	1.00	0.16
	980–1170	8.47	1.38

[a] Temperature interval of the reduction steps.
[b] Weight loss during each reduction stage.
[c] Calculated from: $\delta = [\Delta m MG(AFeO_3)]/[m_0 MG(O)]$, where Δm is the sample weight loss, m_0 is the initial sample weight, $MG(AFeO_3)$ is the molecular weight of the perovskite and MG(O) = 16.

However, only with $GdFeO_3$ and $NdFeO_3$ the last reduction step was completed below 1170 K. XRD patterns of the samples after the first reduction step showed a structure identical to the parent perovskites. After heating to 1170 K, reflections corresponding to the simple lanthanide oxides (A_2O_3) and metallic Fe were detected, and for $LaFeO_3$ also high intensity reflections of the perovskite phase. The change in the non-stoichiometry (δ) after each reduction step has been calculated from the weight loss, according to the formula: $\delta = [\Delta m MG(AFeO_3)]/[m_0 MG(O)]$, where Δm is the sample weight loss, m_0 is the initial sample weight, $MG(AFeO_3)$ is the molecular weight of the perovskite and $MG(O) = 16$. The change in the non-stoichiometry after the first reduction step was specially marked for the $LaFeO_{3+x}$ sample.

Tascón et al. [15] have reported the formation of $LaFeO_{3.18}$ after calcination at 923 K. Although in our study the formation of oxidative non-stoichiometric compounds in the $AFeO_3$ series has not been further investigated, it is possible that, comparable to $AMnO_3$ perovskites, the first reduction step of these rare-earth orthoferrites originates from the reduction of the non-stoichiometric phase. It is important to note that this reduction process requires the diffusion of oxygen ions into the surface, which is a slow process. Consequently surface-near domains can undergo full reduction of the Fe^{3+} ions. The change in the non-stoichiometry reported in table 3 does probably not correspond to the values which are needed for the formation of the stoichiometric phases.

In contrast to $ACoO_3$ [10], $LaNiO_3$ [16] and $LaMnO_3$ [17], the reduction in a hydrogen atmosphere of Fe^{3+} to metallic Fe in $AFeO_{3.00}$ occurred in one step, without formation of an intermediate perovskite-related structure containing Fe^{2+} ions.

3.4. CATALYTIC ACTIVITY

Preliminary tests carried out with 0.100 g of SiO_2 under the same reaction conditions as used for the activity tests, showed negligible CH_4 conversion below 1000 K. At 1100 K predominantly H_2O (710 ppm), CO (260 ppm) and CO_2 (110 ppm) were formed.

To determine the possibility of pore diffusion resistance under reaction conditions, diagnostic tests were performed with $LaMnO_3$ and $PrFeO_3$. The methane conversions, generally below 20%, did not change for both samples when different sieve fractions (50–120, 120–300 and 300-500 μm) were used, indicating that intraparticle diffusion did not affect significantly the overall reaction rate.

Methane conversion versus temperature plots over the $AMnO_{3+x}$ and $AFeO_{3+x}$ catalysts are shown in figs. 5a and 5b, respectively. The catalytic activities were compared at a constant GHSV of 135 000 h^{-1}. Below 650 K virtually no activity was detected over both perovskite systems. The four rare-earth manganites yielded comparable overall activities, a similar behavior was observed with the orthoferrites. Data characterizing the activity, such as reaction rates, temperatures

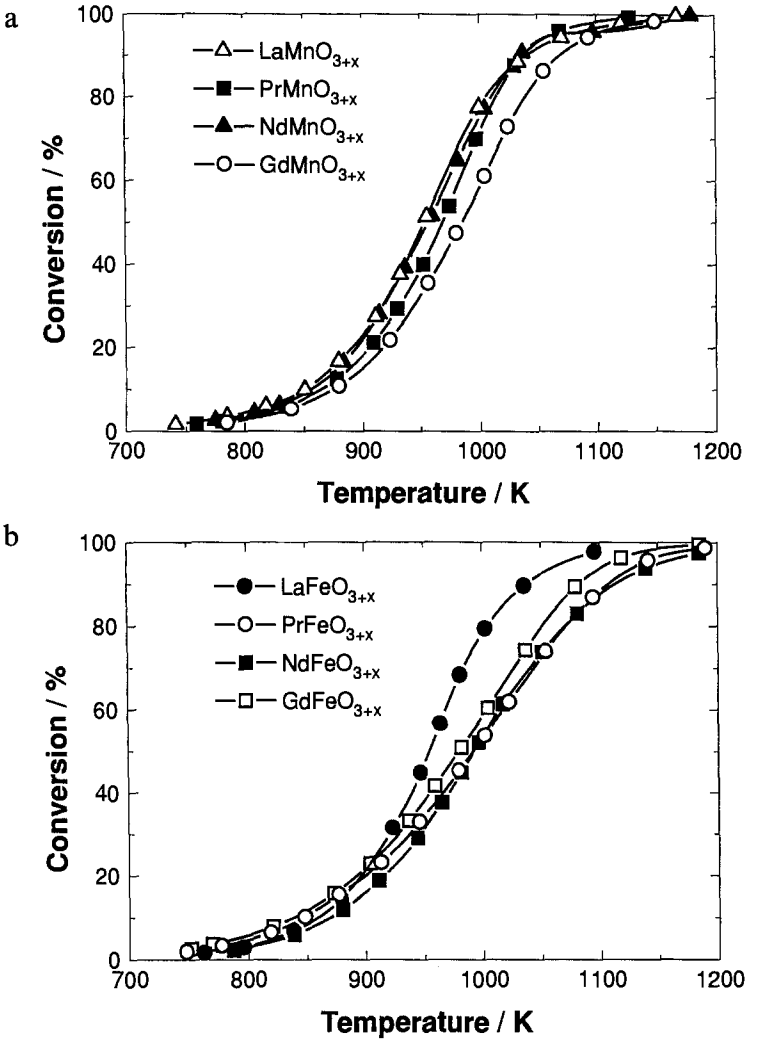

Fig. 5. Comparison of the overall activities of the $AMnO_3$ (a) and $AFeO_3$ (b) catalysts. Reactant gas composition: 1% CH_4, 4% O_2, He (balance); sample weight: 0.1 g; GHSV: 135 000 h^{-1}.

at which 50% of methane conversion is attained ($T_{50\%}$) and apparent activation energies (E_a), are summarized in table 1. The apparent activation energies were determined at conversions below 10%. The $AMnO_{3+x}$ catalysts have activation energies which deviate from each other by maximal 10 kJ mol^{-1}, whereas the $LaFeO_{3+x}$ catalysts show a maximal difference (23 kJ mol^{-1}). The reason for this behavior is presently not understood. The reaction rates, referred to the BET surface areas, measured at 770 K were found to vary between 1.4×10^{-7} and 2.9×10^{-7} mol s^{-1} m^{-2} for the $AMnO_{3+x}$ system, and between 1.1×10^{-7} and 1.6×10^{-7} mol s^{-1} m^{-2} for the $AFeO_{3+x}$ system. A comparison of the Arrhenius plots is shown in fig. 6.

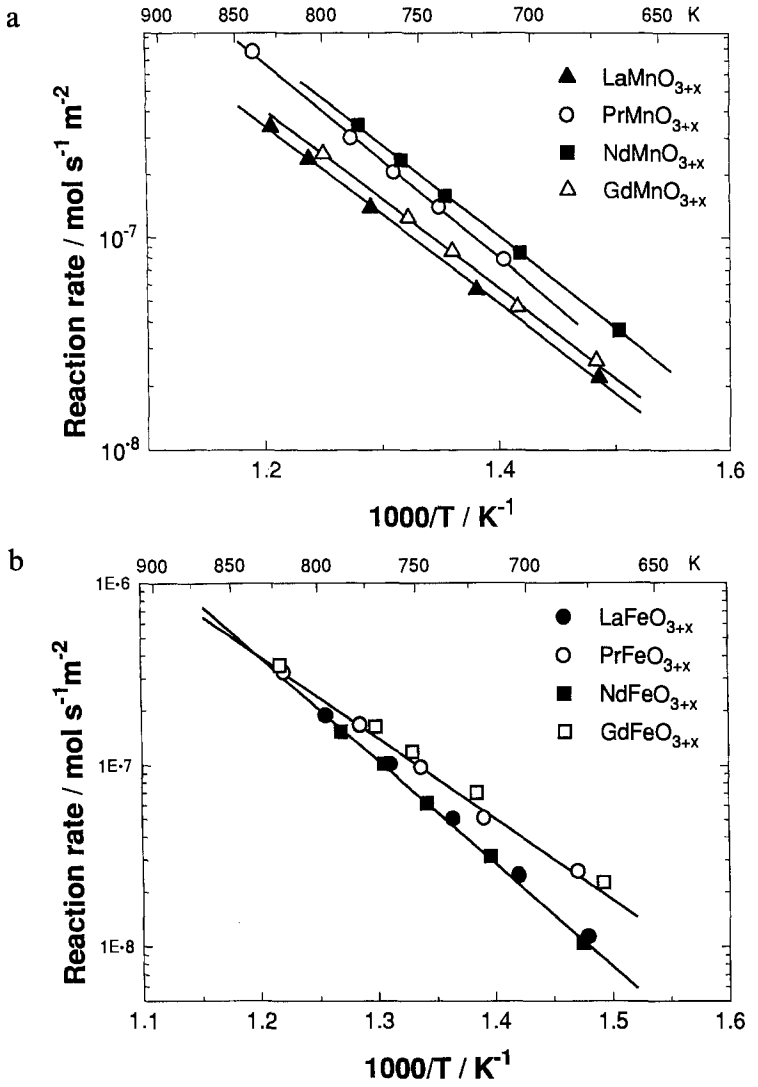

Fig. 6. Arrhenius plots of methane combustion over $AMnO_3$ (a) and $AFeO_3$ (b) catalysts. Reactant gas composition: 1% CH_4, 4% O_2, He (balance); sample weight: 0.1 g; GHSV: 135 000 h^{-1}.

Kinetic measurements were also carried out with Pr_6O_{11} and Gd_2O_3, which were present as impurities in the Pr- and Gd-containing perovskites, respectively. These measurements allowed to estimate the contribution of the simple oxide impurities to the activity of the corresponding perovskites. The oxides, Pr_6O_{11} and Gd_2O_3 from Fluka, were calcined at 1220 K for 8 h, prior to the measurements. The reaction rate of Pr_6O_{11} (BET surface area = 1.8 m^2/g), measured at 770 K, was 3.1×10^{-8} mol s^{-1} m^{-2}, whereas the activity of Gd_2O_3 (BET surface area = 2.5 m^2/g) was 3.3×10^{-9} mol s^{-1} m^{-2}. These results indicate that the impurities had no major influence on the activity of the perovskites.

4. Discussion

The non-stoichiometric behavior characteristic for some ABO_3 perovskites, has been thoroughly investigated [12,17–21]. The oxidative non-stoichiometry in $LaMnO_{3+x}$ is caused by the oxidation of some Mn^{3+} to Mn^{4+}. The stoichiometry can be changed by partial substitution of the A site or by varying the firing conditions. Tofield and Scott [21] have reported for $LaMnO_{3+x}$ a dependence of the stoichiometry on the calcination conditions: low calcination temperatures together with high oxygen partial pressure yielded samples with high oxidative non-stoichiometry, i.e., $LaMnO_{3.20}$ after treatment at 870 K and 130 atm O_2.

In our work, $AMnO_{3+x}$ samples with an oxidative non-stoichiometry have been prepared. The excess of oxygen in the samples was determined from the oxygen evolution experiments (fig. 3, table 2). They show that the nature of the lanthanide ions influences the thermal behavior of these rare-earth manganites. The position of the first desorption step in the TPD profiles varied between 900 K, for $PrMnO_{3+x}$ and 1260 K, for $GdMnO_{3+x}$. After this first event, stoichiometric perovskite phases were formed, as revealed by XRD. The chemical formula of the non-stoichiometric phases resulting under our preparation conditions (1170 K, 1 atm air), as determined by TPD are: $LaMnO_{3.14}$, $PrMnO_{3.05}$, $NdMnO_{3.06}$ and $GdMnO_{3.10}$.

Tofield and Scott [21] investigated the structure of $LaMn^{3+}_{0.76}Mn^{4+}_{0.24}O_{3.12}$ by means of powder neutron diffraction, and suggested the composition $(La_{0.94\pm0.02}\square_{0.06\pm0.02})(Mn^{3+}_{0.745}Mn^{4+}_{0.235}\square_{0.02})O_3$ with partial elimination of La_2O_3 and formation of vacancies ($\square$) on both A and B cation sites. This indicates that the formation of cation vacancies instead of interstitial oxygen is responsible for the excess of oxygen.

Heating the samples at temperatures above 1300 K produces a phase segregation with concomitant formation of the simple oxides.

The $AFeO_3$ samples showed no oxygen evolution up to 1400 K. The high stability of $LaFeO_3$ compared with $LaCoO_3$, $LaNiO_3$ and $LaMnO_3$ has been reported by Nakamura et al. [22]. The comparative study of the reduction behavior of these rare-earth orthoferrites has been carried out with hydrogen as reducing agent. The reductions of the four samples under a hydrogen atmosphere exhibit two steps. XRD patterns of the samples after heating them in hydrogen till completion of the first event, showed the same structure as the parent perovskites. Reduction up to 950 K led to the formation of the lanthanide oxides and metallic Fe. For $LaFeO_3$ the reduction was not complete. A similar behavior has been reported by Tascón et al. [15] for the reduction of $LaFeO_{3.18}$ in hydrogen, the first event was attributed to the reduction of the non-stoichiometric compound to a stoichiometric one, whilst during the second reduction step Fe^{3+} is reduced to metallic Fe. The reducibility of the $AFeO_3$ perovskites, i.e. the temperature at which the reduction process begins, correlates inversely with the relative effective ionic radii (with coordination number 12) of the trivalent rare-earth cations. This is in agreement with the

reported increase of the thermal stability of the perovskite structure with increasing size of the lanthanide ion [23].

The surface area specific reaction rates determined for the oxidation of methane over $AMnO_3$ varies between 1.4×10^{-7} mol s^{-1} m^{-2}, for $LaMnO_3$, and 2.9×10^{-7} mol s^{-1} m^{-2}, for $NdMnO_3$. Also the overall activities are very close to each other (maximal difference of $T_{50\%}$ only 34 K). The kinetic results of the $AFeO_3$ perovskites indicate that the A-site cation has practically no influence on the catalytic activity. The surface area specific reaction rates, measured at 770 K, vary between 1.1×10^{-7}, for $LaFeO_3$, and 1.6×10^{-7} mol s^{-1} m^{-2}, for $GdFeO_3$. Arakawa et al. [24] found for the oxidation of methanol over $AFeO_3$ (A = La–Gd) perovskite-type oxides a marked dependence of the overall activity on the rare-earth ion. However, since no surface area data were reported it is not easy to assign the effective influence of the lanthanide ions on the catalytic activity of these orthoferrites.

Although the ionic radii and charge densities of the lanthanides change from lanthanum to gadolinium (ionic radii of the trivalent lanthanides decrease with increasing atomic number), and consequently also the perovskite structure, it can be concluded from our results that the deep oxidation of methane over both of these perovskite systems is insensitive to the A-site cation. This is in agreement with the results reported by Nitadori et al. [8] for the oxidation of propane and methanol over ABO_3 perovskites, and the results of Baiker et al. [10] for the oxidation of methane over $ACoO_3$ perovskites. In the latter work, the reaction rates at 770 K, measured under the same conditions as used in the present work, were: 1.9×10^{-7} mol s^{-1} m^{-2}, for $GdCoO_3$, 1.6×10^{-7} mol s^{-1} m^{-2}, for $NdCoO_3$, 1.2×10^{-7} mol s^{-1} m^{-2}, for $LaCoO_3$, which is about 30 times higher than that measured with $PrCoO_3$. The low activity of $PrCoO_3$ was attributed to the presence of Co^{2+} ($Pr^{3+}_{1-x}Pr^{4+}_{x}Co^{3+}_{1-x}Co^{2+}_{x}O_3$).

5. Conclusions

$AMnO_{3+x}$ perovskites with oxidative non-stoichiometry ($LaMnO_{3.14}$, $PrMnO_{3.05}$, $NdMnO_{3.06}$ and $GdMnO_{3.10}$) have been prepared. Thermal reduction leads first to the formation of the corresponding stoichiometric phases. $AFeO_{3+x}$ perovskites are thermally more stable than the manganites. The reduction of Fe^{3+} to metallic Fe in $AFeO_{3.00}$ occurs in one step, without formation of an intermediate perovskite-related structure containing Fe^{2+} ions. The A-site cations have only insignificant influence on the catalytic activity for methane oxidation.

Acknowledgement

We thank the Bundesamt für Energiewirtschaft (BEW) for financial support of this work. Helpful discussions with Dr. Heiko Viebrock are gratefully acknowledged.

References

[1] D.L. Trimm, Appl. Catal. 7 (1983) 249.
[2] R. Prasad, L.A. Kennedy and E. Ruckenstein, Catal. Rev.-Sci. Eng. 26 (1984) 1.
[3] L.D. Pfefferle and W.C. Pfefferle, Catal. Rev.-Sci. Eng. 29 (1987) 219.
[4] J.P. Kesselring, in: *Advanced Combustion Method*, ed. F.J. Weinberg (Academic Press, London, 1986).
[5] H. Arai and M. Machida, Catal. Today 10 (1991) 81.
[6] H. Arai, T. Yamada, K. Eguchi and T. Seiyama, Appl. Catal. 26 (1986) 265.
[7] J.G. McCarty and H. Wise, Catal. Today 8 (1990) 231.
[8] T. Nitadori, T. Ichiki and M. Misono, Bull. Chem. Soc. Japan 61 (1988) 621.
[9] H.M. Zhang, Y. Shimizu, Y. Teraoka, N. Miura and N. Yamazoe, J. Catal. 121 (1990) 432.
[10] A. Baiker, P.E. Marti, P. Keusch, E. Fritsch and A. Reller, J. Catal. (1993), in press.
[11] K.R. Barnard, K. Foger, T.W. Turney and R.D. Williams, J. Catal. 125 (1990) 265.
[12] A. Wold and R.J. Arnott, J. Phys. Chem. 9 (1959) 176.
[13] K.S.W. Sing, D.H. Everett, R.A.W. Haul, L. Moscou, Pierotti, J. Rouquérol and T. Siemieniewska, Pure Appl. Chem. 57 (1985) 603.
[14] S. Quezel-Ambrunaz, Bull. Soc. Fr. Minéral. Cristallogr. 91 (1968) 339.
[15] J.M.D. Tascón, J.L.G. Fierro and L.G. Tejuca, J. Chem. Soc. Faraday Trans. 81 (1985) 2399.
[16] M. Crespin, L. Gatineau, J. Fripiat, H. Nijs, J. Marcos and E. Lombardo, Nouv. J. Chim. 7 (1983) 477.
[17] M.L. Rojas, J.L.G. Fierro, L.G. Tejuca and A.T. Bell, J. Catal. 124 (1990) 41.
[18] C.N.R. Rao and J. Gopalakrishnan, *New Directions in Solid State Chemistry* (Cambridge Univ. Press, Cambridge, 1986).
[19] K. Kamata, T. Nakajima, T. Hayashi and T. Nakamura, Mates. Res. Bull. 13 (1978) 49.
[20] M. Seppänen, Kytö and P. Taskinen, Scand. J. Metall. 9 (1980) 3.
[21] B.C. Tofield and W.R. Scott, J. Solid State Chem. 10 (1974) 183.
[22] T. Nakamura, G. Petzow and L.J. Gauckler, Mater. Res. Bull. 14 (1979) 649.
[23] T. Arakawa, N. Ohara and J. Shiokawa, Chem. Lett. (1984) 1467.
[24] T. Arakawa, S. Tsuchi-ya and J. Shiokawa, J. Catal. 74 (1982) 317.